A CALCULATION OF THE FLUX AND ENERGY SPECTRUM OF SECONDARY ELECTRONS AT HIGH ALTITUDES IN THE ATMOSPHERE*

Satya Dev Verma**

Enrico Fermi Institute for Nuclear Studies
and Department of Physics
The University of Chicago

Laboratory for Astrophysics and Space Research

Preprint No. EFINS 66-44

May 1966

*Work supported by the National Aeronautics and Space Administration under grant NASA NsG 144-61.

**On leave from Tata Institute of Fundamental Research, Bombay, India

A CALCULATION OF THE FLUX AND ENERGY SPECTRUM OF SECONDARY ELECTRONS AT HIGH ALTITUDES IN THE ATMOSPHERE*

Satya Dev Verma**
Enrico Fermi Institute for Nuclear Studies
and Department of Physics
The University of Chicago

ABSTRACT

Calculations are carried out to determine the flux and energy spectra of secondary electrons which are produced by the cosmic radiation in the upper layers of the atmosphere. The calculations are valid to an atmospheric depth of about 10 g/cm^2. Electron spectra are presented for different depths and locations where measurements of the electron flux have been carried out: Ft. Churchill, Manitoba; Sioux Falls, South Dakota, Palestine, Texas; and Hyderabad, India. The calculations are compared with observed electron fluxes during the ascents of balloon flights.

---

*Work supported by the National Aeronautics and Space Administration under grant NASA NsG 144-61

**On leave from Tata Institute of Fundamental Research, Bombay, India.

I. INTRODUCTION

All measurements of the cosmic ray electron component which are carried out at balloon altitude have contributions of secondary electrons and, if made at intermediate or low geomagnetic latitudes, of re-entrant albedo electrons. In this paper we wish to present a calculation of the vertical flux and energy spectra of secondary electrons in the uppermost layers of the atmosphere. Such calculations are useful and necessary for the correction of experimental work obtained on balloons. The accuracy of the calculations is limited by approximations and by the scarcity of detailed experimental data on the production of π-mesons. The results which we report here are estimated to be accurate within about 25%. The approximations used for the calculations will be discussed in the appropriate sections.

The starting point for a calculation of the secondary electron spectrum is the production spectrum of charged and neutral π-mesons in the atmosphere. Two approaches may be used to obtain the spectrum of π-mesons:

1. From experimental work on the energy spectrum of μ-mesons at sea level, underground, and at aircraft altitude the π-meson spectrum may be derived. This method has been used by Sands [1950], Garibian and Goldman [1954], Tulinov [1958], Subramanian and Verma [1959], Pine et al. [1959], Wolfendale [1963] and Tanaka

et al. [1965, private communication]. In Figure 4, such spectra are shown along with the one derived here.

2. The π-meson production spectrum may be calculated directly by using the known primary cosmic ray proton spectrum (Figure 1) and accelerator data for the π-meson production in nuclear interactions between high energy protons and target materials like C, Be, etc. which have Z similar to the nuclei of the atmosphere. In recent years, an increasing amount of such data has become available for protons with energy up to 30 BeV.

In this paper, we use the second approach for a determination of the π-meson production spectrum. This has also been done by Okuda and Yamamoto [1965]. In the energy region where accelerator data are available, the experimental energy distributions and angular distributions of the π-mesons were used and π-meson spectra produced by protons with energies between 1.5 and 30 BeV are derived in Section III. Above 30 BeV there exist no accelerator data and one has to rely on the results of cosmic ray experiments and simplified models for π-meson production. In Section IV, we discuss the π-meson production spectrum originating from protons in the energy range between 30 BeV and a few 1000 BeV. Charged K-mesons, which are all assumed to decay into μ-mesons, are included in the π-meson production

spectrum. We also allow, in an approximate way, for the production of π-mesons by primary cosmic ray α-particles and heavier nuclei.

The secondary electron energy spectrum, arising from the decay of charged pions and muons then is obtained in Section V and the contribution by neutral π-mesons and Dalitz-pairs to the secondary electron component is discussed in Section VI.

Finally, we shall compare the results of our calculations with experimental data on the electron component in the atmosphere which were obtained during balloon ascents at a variety of geomagnetic latitudes.

II. ASSUMPTIONS AND APPROXIMATIONS IN THE CALCULATION

The intensity of the secondary electrons was calculated under the following assumptions:

1. The intensity of the primary cosmic radiation is isotropic, and has a sharp geomagnetic cut-off.
2. Since accelerator data on the energy distribution and the angular distribution of π-mesons are available only for a few discrete proton energies, interpolation for intermediate energies had to be made.
3. Primary particles heavier than protons have been included in the calculations under the simplifying assumption that these nuclei

behave like "A" nucleons in an interaction, where A is the number of nucleons in the primary.

4. The atmosphere was assumed to be isothermal with a constant scale height of 6.46 km.

III. THE VERTICAL INTENSITY OF π-MESONS PRODUCED BY PRIMARY PARTICLES HAVING ENERGY PER NUCLEON BETWEEN 1.5 TO 30 BeV

Let us consider the number of charged π-mesons produced by protons of energy between E_0 and E_1 per unit area at a depth X in a target thickness dX, moving vertically downwards and having energy between E_π and $E_\pi + dE_\pi$. This number is given by

$$\frac{d j_\pi}{dX}(E_\pi, X)\, dE_\pi\, dX = \int_{E_0}^{E_1} J(E_p)\, m(E_p)\, dE_p \int_0^{\theta_p(max)} \left(\frac{N\bar{\sigma}}{\rho}\right) d\Omega(\theta_p)$$

$$\exp\left(-\frac{X}{L_a \cos\theta_p}\right) f(\theta, E_\pi)\, dE_\pi\, dX \qquad \text{---(1)}$$

where $J(E_p)$ is the differential energy spectrum of primary protons (Figure 1) based upon the experimental work of McDonald [1958], Balasubramanyan et al. [1965], Ormes and Webber [1965] and Waddington and Freier [1965] around solar minimum. $m(E_p)$ is the multiplicity for production of the charged π-mesons (Figure 2) in nuclear interactions between high energy

protons and target materials like C, Be, etc. which have similar Z to the nuclei of the atmosphere. This multiplicity was obtained from the work of Pollack and Fazio [1961], Lal et al. [1962] and Melhotra [1963]. Furthermore, $d\Omega(\theta_p)$ is the element of solid angle at θ_p from the Zenith and $d\Omega(\theta)$ is the element of solid angle in the vertical direction looking downwards. This is considered to be the direction of the secondary particle (see Fig. 3), and θ is the angle between primary and secondary directions. As is clear from Figure 3, θ and θ_p are equal in our case. L_a is the absorption mean free path in (g/cm^2) of protons in air, N is the number of atoms per unit volume, $\bar{\sigma}$ is the total production cross-section for the production of charged π-mesons, and ρ is the density of air. The function $f(\theta, E_\pi)$ represents the normalized energy and angular distribution of π-mesons in the laboratory system, obtained by using the data on π-meson production in accelerator experiments of Melissinos et al. [1962], Lundy et al. [1965] and Dekkers et al. [1965] such that

$$\int_{4\pi} \int_{0}^{\infty} f(\theta, E_\pi)\, d\Omega(\theta)\, dE_\pi = 1 \qquad \text{- - -} \quad (2)$$

We know that $\bar{\sigma}$ is a slowly varying function of E_p. Here $\bar{\sigma}$ is considered constant and its variation as a function of E_p is taken into account in $m(E_p)$ (Figure 2). Now we put $\frac{N\bar{\sigma}}{\rho}$ = constant = $\frac{1}{L_i}$; where L_i is the

interaction mean free path of protons (70 g/cm^2). In order to estimate the contribution of π-mesons produced by primary particles heavier than protons, we multiply the above equation by a constant α, where α is estimated to be 1.84 ± 0.28.

$$\frac{dJ_1}{dx}(E_\pi, x)\, dE_\pi\, dx = \alpha \frac{dj_1}{dx}(E_\pi, x)\, dE_\pi\, dx \qquad \text{---(3)}$$

Equation (3) can be rewritten as

$$\frac{dJ_1}{dx}(E_\pi, x)\, dE_\pi\, dx = \frac{F_1(E_\pi)}{L_i} \exp\left(-\frac{x}{L_a}\right) dx\, dE_\pi \qquad \text{---(4)}$$

where

$$F_1(E_\pi) = 2\pi\alpha \int_{E_0}^{E_1} J(E_p)\, m(E_p)\, dE_p \int_0^{\theta_p(max)} \sin\theta_p\, f(\theta_p, E_\pi) \exp\left[-\frac{x(1-\cos\theta_p)}{L_a \cos\theta_p}\right] d\theta_p \qquad \text{---(5)}$$

Since we are interested in an evaluation of the π-meson flux for the upper 10 g/cm^2 of the atmosphere only, we have $\frac{X}{L_a} \ll 1$. And, in addition, we have only to consider incident particles within a zenith angle of about 60°. Therefore, $0 \leq \theta_p \leq 60^\circ$, which leads to $\exp\left[-\frac{X(1-\cos\theta_p)}{L_a \cos\theta_p}\right] \simeq 1$ within 7% since $L_a = 120$ g/cm^2. Hence, Eq. (5) becomes

$$F_1(E_\pi) = 2\pi\alpha \int_{E_0}^{E_1} J(E_p)\, m(E_p)\, dE_p \int_0^{\theta_p(max)} \sin\theta_p\, f(\theta_p, E_\pi)\, d\theta_p \qquad \text{---(6)}$$

$F_1(E_\pi)$, the π-meson production spectrum, is the intensity of π-mesons produced if all the primary particles having energy per nucleon between E_0 and E_1 do interact with air nuclei.

IV. THE VERTICAL INTENSITY OF π-MESONS PRODUCED BY PRIMARY PARTICLES HAVING ENERGY PER NUCLEON BETWEEN 30 TO 1000 BeV

Equation (6) derived in the previous section for the π-meson production spectrum, can be used only when the function $f(\theta_p, E_\pi)$ is known, preferentially from experiment. Because of the absence of data above 30 BeV proton energy, the useful approximation is to assume that all the π-mesons are produced in a narrow cone in the forward direction in the Lab. system. In the experimental work of Iwadare [1959], Azimov et al. [1963], Hildebrand and Silberberg [1963], Lal et al. [1963], Lock [1963], Abraham et al. [1965] Babayan, et. al. [1965] and Grigorov et al. [1965] it was found that the π^o inelasticity, i.e., the fraction of primary energy going into π^o-mesons, is 0.15 ± 0.06. It was also shown that the inelasticity for production of charged π-mesons is twice that of π^o-mesons.

For simplicity, we assume that all the π-mesons have equal energy.

Then for charged π-mesons

$$E_\pi = \frac{E_p K(E_p)}{m(E_p)} \qquad \text{---(7)}$$

where $K(E_p)$ and $m(E_p)$ are the inelasticity and the multiplicity of charged π-mesons in nuclear interactions with protons.

The number of charged π-mesons produced per unit area at a depth X in a target thickness dX, moving vertically downwards and having an energy between E_π and $E_\pi + dE_\pi$ by particles having energy per nucleon between E_1 and E_2 is given by

$$\frac{dJ_2}{dX}(E_\pi, X)\,dE_\pi\,dX = \frac{\alpha}{L_i}\int_{E_1}^{E_2} J(E_p)\,m(E_p)\frac{dE_p}{dE_\pi}\exp\left(-\frac{X}{L_a}\right)dX\,dE_\pi \;\delta\left(E_p - E_\pi\, m(E_p)/K(E_p)\right) \qquad \text{---(8)}$$

or

$$\frac{dJ_2}{dX}(E_\pi, X)\,dE_\pi\,dX = \frac{F_2(E_\pi)}{L_i}\exp\left(-\frac{X}{L_a}\right)dE_\pi\,dX \qquad \text{---(9)}$$

where

$$F_2(E_\pi) = \left[\alpha\, J(E_p)\, m(E_p)\frac{dE_p}{dE_\pi}\right], \text{ with } E_p = E_\pi\frac{m(E_p)}{K(E_p)} \qquad \text{---(10)}$$

or

$$F_2(E_\pi) = \left[\frac{\alpha J(E_p)\, m^2(E_p)}{K(E_p)} \right] \quad \text{---(10')}$$

Thus by adding Eqs. (6) and (10') we get the production spectrum of charged π-mesons over the entire energy region:

$$F(E_\pi) = F_1(E_\pi) + F_2(E_\pi) \quad (11)$$

By choosing E_0 corresponding to the geomagnetic cut-off rigidity at different locations on the earth, we derived the production spectrum of charged π-mesons for Fort Churchill, Canada; Sioux Falls, South Dakota; Palestine, Texas; and Hyderabad, India (Figure 4).

Using the assumption that the multiplicity for π^o-meson production is one-half that for charged π-mesons, we get the production spectrum of the neutral π-mesons from Eq. (11) by dividing it by 2.

V. THE DIFFERENTIAL ENERGY SPECTRA OF SECONDARY ELECTRONS FROM CHARGED π-MESONS

The sum of Equations (4) and (9) yields, within our approximation, the spectrum of charged π-mesons produced at a depth X and thickness dX having energy between E_π and $E_\pi + dE_\pi$.

$$\frac{dJ}{dx}(E_\pi, x)\,dE_\pi\,dx = \left\{F_1(E_\pi) + F_2(E_\pi)\right\} \exp\left(-\frac{x}{L_a}\right)\frac{dx}{L_i}\,dE_\pi$$

$$= F(E_\pi)\exp\left(-\frac{x}{L_a}\right)\frac{dx}{L_i}\,dE_\pi \qquad \text{---(12)}$$

The energy spectrum of the charged π-mesons which are produced above a depth X_1 and decay between X_1 and $X_1 + dX_1$ is given by

$$\frac{dF}{dX_1}(E_\mu, X_1)\,dE_\mu = \frac{F(E_\pi)\,dE_\pi}{L_i\,dE_\mu}\int_0^{X_1} \exp\left(-\frac{x}{L_a}\right) p(x, X_1)\,dx\,dE_\mu \qquad \text{---(13)}$$

This is also the production spectrum of μ-mesons, since the π-mesons decay into muons. (We have neglected collisions of π-mesons due to the low density of the medium and have assumed that all μ-mesons maintain the direction of the pions.) $p(X, X_1)$ is the probability that a charged π-meson which was produced at a depth X will decay between X_1 and $X_1 + dX_1$

$$p(x, x_1) = \frac{d}{dx_1}\left[1 - \exp\left\{-\frac{y(x) - y(x_1)}{c\,\tau_\pi\,\gamma_\pi}\right\}\right]$$

$$= \frac{d}{dx_1}\left[1 - \exp\left\{-\frac{y(x) - y(x_1)}{H_0}\,h\right\}\right] \qquad \text{---(14)}$$

where τ_π is the π-meson lifetime in its rest frame

γ_π is the π-meson Lorentz factor

and y(x) is the height in cm above sea level at an atmospheric depth X (g/cm^2). We assume a standard atmosphere where

$$X = X_0 \exp\left(-\frac{y(X)}{H_0}\right) \qquad \text{---} \quad (15)$$

and H_0 is the height of the standard atmosphere = 6.46×10^5 cm [Grigorov, 1956]. We define

$$h = \frac{H_o}{c\tau_\pi \gamma_\pi} = \frac{H_o m_\pi c^2}{c\tau_\pi E_\pi} = \frac{118}{E_\pi} \quad : \quad E_\pi \text{ in BeV.}$$

Combining Eqs. (14) and (15) we get

$$p(X,X_1) = \frac{d}{dX_1}\left[1 - \left(\frac{X}{X_1}\right)^h\right] = \frac{hX^h}{X_1^{h+1}} \qquad \text{---} \quad (16)$$

Substituting p(X, X_1) in Eq. (13) we obtain the muon production spectrum

$$\frac{dF}{dX_1}(E_\mu, X_1)\,dE_\mu = \frac{F(E_\pi)}{L_i}\frac{dE_\pi}{dE_\mu}\int_0^{X_1} \exp\left(-\frac{x}{L_a}\right)\frac{h\,x^h}{X_1^{h+1}}\,dx\,dE_\mu \qquad \text{---} \quad (17)$$

and, since $\frac{X_1}{L_a} \ll 1$, we get

$$\frac{dF}{dX_1}(E_\mu, X_1)\,dE_\mu = \left\{\frac{F(E_\pi)}{L_i}\frac{dE_\pi}{dE_\mu}\left(\frac{h}{h+1}\right)\left(1 - \frac{X_1(h+1)}{L_a(h+2)}\right)\right\} dE_\mu \qquad \text{---} \quad (18)$$

This is the number of muons produced per cm^2 per sec at depth X_1 in thickness dX_1 having energy between E_μ and $E_\mu + dE_\mu$.

The probability that a muon produced at a depth X_1 will have decayed into an electron before it reaches a depth X_2 is given by

$$W(X_1, X_2) = 1 - \exp\left(-\frac{y(X_1) - y(X_2)}{H_0} g\right)$$
$$= 1 - \left(\frac{X_1}{X_2}\right)^g \quad \text{---} \quad (19)$$

where $g = \dfrac{H_o\, m_\mu c^2}{c\tau_\mu E_\mu} = \dfrac{1.07}{E_\mu}$; E_μ in BeV.

τ_μ, E_μ are the lifetime and the energy of the muons.

The number of decayed muons at a depth X_2, i.e., the number of electrons at a depth X_2 due to muon decay is given by

$$J(E_e, X_2)dE_e = \int_0^{X_2} dF(E_\mu, X_1)\frac{dE_\mu}{dE_e}\left\{1 - \left(\frac{X_1}{X_2}\right)^g\right\} dX_1\, dE_e$$
$$= \frac{F(E_\pi)}{L_i}\frac{dE_\pi}{dE_e}\frac{h}{(h+1)}\int_0^{X_2}\left\{1 - \left(\frac{X_1}{X_2}\right)^g\right\}\left\{1 - \frac{X_1(h+1)}{L_a(h+2)}\right\} dX_1\, dE_e$$

Solving, we get

$$J(E_e, X_2)dE_e = \frac{F(E_\pi)}{L_i}\frac{dE_\pi}{dE_e}\frac{h}{(h+1)}\frac{g}{(g+1)}\left[1 - \frac{X_2(h+1)(g+1)}{2L_a(h+2)(g+2)}\right] dE_e \quad \text{---} \quad (20)$$

Since we are interested in $X_2 \ll L_a$ and $E_\pi \lesssim 10$ BeV, $\frac{h}{h+1} \cong 1$ and

$$\frac{X_2(h+1)(g+1)}{2L_a(h+2)(g+2)} \ll 1 ,$$

we may simplify Equation (20):

$$J(E_e, X_2) = \frac{F(E_\pi)}{Li} \frac{dE_\pi}{dE_e} \frac{h}{(h+1)} \frac{g}{(g+1)} X_2 \text{ ---} (24)$$

The above approximations produce an error of about 10 %. The average value of the factor $[F(E_\pi) \frac{dE_\pi}{dE_e}]$ is calculated using the data of Scanlon and Milford [1965] on the π-μ-e decay and the production spectrum $F(E_\pi)$ given in Figure 4 in deriving the electron energy spectrum due to decay of charged π-mesons. The results for $J(E_e, X_2)$ in the case of $X_2 = 1$ g/cm^2 is shown in Figure 5 at different geomagnetic cut-offs.

VI. THE DIFFERENTIAL ENERGY SPECTRUM OF SECONDARY ELECTRONS FROM NEUTRAL π-MSEONS

It was pointed out in Section IV that the production spectrum for neutral π-mesons may be obtained by dividing Eq. (11) by 2. Since their lifetime is very small (10^{-15} sec), they decay immediately into two gamma rays, with average energy $\bar{E}_\gamma = 1/2\, E_\pi$ o. Therefore, the production

spectrum for gamma rays is given by

$$\frac{dF}{dx}(\bar{E}_\gamma, X)\, d\bar{E}_\gamma = \frac{2F(E_\pi)}{2L_i}\frac{dE_\pi^\circ}{dE_\gamma} \exp\left(-\frac{X}{L_a}\right) d\bar{E}_\gamma$$

$$= \frac{2F(E_\pi)}{L_i} \exp\left(-\frac{X}{L_a}\right) d\bar{E}_\gamma \quad \text{---(22)}$$

The gamma rays in most cases produce two pairs of electrons. The characteristic length for pair production is $L_\gamma = 50$ g/cm^2 in the air. We also assume $\bar{E}_e = 1/2\, \bar{E}_\gamma$. Therefore, the electron spectrum at depth X_2 can be written as

$$J(\bar{E}_e, X_2)\, d\bar{E}_e = 2\int_0^{X_2} \frac{dF}{dx}(\bar{E}_\gamma, X)\frac{d\bar{E}_\gamma}{d\bar{E}_e}\, dx \left[1 - \exp\left(-\frac{X_2 - X}{L_\gamma}\right)\right] d\bar{E}_e$$

$$= 4\int_0^{X_2} \frac{F(E_\pi)}{L_i} \exp\left(-\frac{X}{L_a}\right)\left[1 - \exp\left(-\frac{X_2 - X}{L_\gamma}\right)\right]\frac{d\bar{E}_\gamma}{d\bar{E}_e}\, dx\, d\bar{E}_e$$

$$= \frac{8F(E_\pi)}{L_i}\int_0^{X_2} \exp\left(-\frac{X}{L_a}\right)\left[1 - \exp\left(-\frac{X_2 - X}{L_\gamma}\right)\right] dx\, d\bar{E}_e$$

Expanding the term inside the integral and keeping terms up to third order in $\left(\frac{X_2 - X}{L_\gamma}\right)$ we get

$$J(\bar{E}_e, X_2) = \frac{4F(E_\pi)}{L_i L_\gamma} X_2^2 \left[1 - \frac{X_2(L_a + L_\gamma)}{3 L_a L_\gamma}\right] \quad \text{---(23)}$$

The second term in the square brackets is much smaller than 1: $\frac{X_2(L_a + L_\gamma)}{3L_a L_\gamma} \ll 1$

and we therefore neglect it. The error due to this approximation is also $\leq$ 10%. The secondary electrons produced by Dalitz pairs amount to 1.2% of the π^{o}-meson flux at all energies.

VII. RESULTS AND DISCUSSION

The secondary electron spectrum is given by the sum of Equations (21) and (23). Both the shape of the spectrum and the total electron flux depend upon the flux of protons incident on the atmosphere and are therefore a function of geomagnetic latitude. We have evaluated the secondary electron spectrum for some of the locations on the earth where electrom measurements were carried out at balloon altitudes. We chose Ft. Churchill, Manitoba; Sioux Falls, South Dakota; Palestine, Texas and Hyderbad, India. The vertical geomagnetic cutoffs according to Quenby and Wenk [1962] are 0.19, 1.6, 4.9 and 16 Bv respectively. In Figs. 5 and 6, we show separately the flux of secondary electrons due to π-μ-decay, due to π^{o}-mesons and due to Dalitz-pairs as a function of energy and for an atmospheric depth of 1 g/cm^{2}. Figs. 7 through 10 show the total flux of secondary electrons as a function of energy at various depths in the atmosphere, again for the four locations mentioned above. In view of the approximations that were used in deriving these spectra and the uncertainties in the available data, we estimate an accuracy of about 25%.

It is desirable to compare the results which were obtained in this work with experimental data. This cannot be done directly, since, as was mentioned above, all measurements of the vertical flux of electrons contain either primary electrons or return albedo electrons in addition to the secondaries. It is, however, possible to compare the measured altitude dependence of the flux of electrons with the results of the calculation. This comparison was done in the following way. The electron energy spectrum as measured at floating altitude during several balloon flights (typically between 3 and 5 g/cm^2) was corrected for secondaries, using the results of this paper, and extrapolated to the top of the atmosphere. An absorption curve for the incident electrons (primary and/or re-entrant albedo) was calculated. The fluxes of the incident electrons and the calculated secondary electrons were then added at each depth up to 30 g/cm^2 and compared with the measured electron flux as a function of atmospheric depth. The result of this procedure is shown in Figs. 11 through 14 for various energy intervals, various locations and different times using experimental data of Meyer and Vogt [1961] Vogt [1962], L'Heureux [1966] and Verma [1966]. At float altitude, the calculated curve and the measured flux are matched by the procedure which was used here. The shape of the calculated altitude curve fits the experimental data well to about 30 g/cm^2. It should be noted that the altitude

curve for the secondaries has not been adjusted or normalized. The Churchill data of Meyer and Vogt [1961] were taken two years after solar maximum [1960]. Therefore, to compare the calculations with their data, we reduced the calculated secondary electron flux by about 40%, which is roughly the change in primary proton intensity. The Sioux Falls data of Vogt [1962] were taken in 1962 and the change in proton flux above 1.6 B_V from 1962 to 1965 was less than 15%. Since the uncertainty in the calculation is about 25% and there are additional errors in the experimental data, we did not attempt to correct for this change in primary intensity. This comparison with the experimental data is not a very stringent test for the accuracy of the calculations; it shows, however, that the calculations do not contradict the observations. More accurate measurements of the altitude dependence of the electron flux in various energy intervals would be desirable.

The author gratefully acknowledges inspiring discussions with Dr. P. Meyer and Mr. J. L'Heureux. He wishes to express his thanks to Dr. R. Vogt and Mr. L'Heureux for permission to use their unpublished data in this paper. He is greatly indebted to Messrs. L. Hecht and R. Ekstrom for their help in the computational work.

REFERENCES

Abraham, F., J. Gerula, R. Levi Setti, K. Rybicki, C. H. Tsao, W. Wolter, R. L. Fricken, and R. W. Huggett, Multiple Meson Production by Heavy Primary Nuclei of Cosmic Origin and Their Fragmentation Products at Energies about 10^{12} eV, Enrico Fermi Institute Report EFINS 65-44, 1965.

Azimov, S. A., A. M. Abdullaev, V. M. Myalkovsky, and T. S. Yuldashev, Investigation of Inelasticity at Interaction of Particles with Nuclei in 70 - 700 GeV Energy Region, Int. Conf. on Cosmic Rays, (Jaipur, India), 5, 69-73, 1963.

Babayan, Kh. P., N. L. Grigorov, E. A. Mamijenyan, and V. Ya Shestoperov, Nuclear Interactions of High Energy With Large Inelasticity, Int. Conf. on Cosmic Rays, (London), 1965.

Balasubramanyan, V. K., D. E. Hagge, G. H. Ludwig, and F. B. McDonald, The Multiply Charged Primary Cosmic Rays at Solar Minimum, 1965, J. Geophys. Res. 71, 1771-1780, 1965.

Dekkers, D., J. A. Geibel, R. Mermod, G. Weber, T.R. Willitts, K. Winter, B. Jordan, M. Vivargent, N. M. King, and E. J. N. Wilson, Experimental Study of Particle Production at Small Angles in Nucleon-Nucleon Collision at 19 and 23 GeV/c, Phys. Rev. 137, B 962-978, 1965.

Garibian, G., and I. Goldman, π - and μ-Mesons in Cosmic Rays, JETP (U.S.S.R.) 26, 256-269, 1954.

Grigorov, N. L., The Average Characteristics of the Interactions of Primary Cosmic Rays of Various Energies (2 - 1000 GeV) With Light Atomic Nuclei, Usp. Fiz. Nauk (U.S.S.R.)58, 599-666, 1956.

Grigorov, N. L., I. N. Erofeeva, L. G. Mitshenko, V. S. Murzin, I. D. Rapoport, L. I. Saritcheva, and G. L. Pashindjagian, The Distribution of Energy Transferred to Neutral Mesons, Int. Conf. on Cosmic Rays, (London) 1965.

Hildebrand, B., and R. Silberberg, Meson Emission Asymmetry, Inelasticity and Multiplicity in Ultra-High Energy Interactions, Int. Conf. on Cosmic Rays, (Jaipur, India) 5, 20 - 25, 1963.

Iwadare, J., On the Elasticity in the High Energy Jet Events, Nuovo Cimento, 12, 630 - 634, 1959.

Lal, S. , Y. Pal, and R. Raghavan, Nuclear Interactions at 20 to 150 GeV in Carbon, Nuclear Physics 31, 415-446, 1962.

Lal, S. , R. Raghavan, T. N. Rangaswamy, A. Subramanian, S. C. Tonwar, and R. H. Vatcha, A Comparison of the Average Characteristics of Nuclear Collisions Produced by Cosmic Ray Particles in Carbon and Brass at Energies ~ 50 GeV, Int. Conf. on Cosmic Rays, (Jaipur, India), 5, 377 - 381, 1963.

L'Heureux, J., Measurement of the Primary Electron Spectrum Near Solar Minimum, (to be published, 1966).

Lock, W. O., Particle Production at GeV Energies, Int. Conf. on Cosmic Rays, (Jaipur, India), 5, 105-140, 1963.

Lundy, R. A., T. B. Novey, D. D. Yovanovich, and V. L. Telegdi, $\pi^{\pm}$ and $K^{\pm}$ Production Cross-sections for 12.5 - BeV Protons on Be, Phys. Rev. Letters, 14, 504-507, 1965.

McDonald, F. B., Primary Cosmic Ray Proton and Alpha Flux Near the Geomagnetic Equator, Phys. Rev. 109, 1367-1375, 1958.

Melhotra, P. K., Dependence of Multiplicity on Primary Energy in Nucleon-Nucleon and Pion-Nucleon Collisions, Nuclear Physics 46, 559-571, 1963.

Melissionos, A. C., T. Yamanouchi, G. G. Fazio, S. J. Lindenbaum, and L. C. L. Yuan, π -Meson Production in 2.9 BeV p-p Collisions, Phys. Rev. 128, 2373-2381, 1962.

Meyer, P. and R. Vogt, Electrons in the Primary Cosmic Radiation, Phys. Rev. Letters, 6, 193-196, 1961.

Okuda, H. and Y. Yamamoto, Cosmic Rays in the Upper Atmosphere, Rep. of Ion. and Sp. Res. in Japan, 19, 322-338, 1965.

Ormes, J. F. and W. R. Webber, Measurement of Primary Proton and Helium Spectra and Their Modulations Using a Balloon-Borne Cerenkov Scintillation Counter, Int. Conf. on Cosmic Rays (London), 1965.

Pine, J., R. J. Davisson, and K. Greisen, Momentum Spectrum and Positive Excess of μ-mesons, Nuovo Cimento 14, 1181-1203, 1959.

Pollack, J. B. and G. G. Fazio, Production of π -Mesons and Gamma Radiation in Galaxy by Cosmic Rays, Phys. Rev. 131, 2684-2691, 1963.

Quenby, J. J. and G. J. Wenk, Cosmic Ray Threshold Rigidities and the Earth's Magnetic Field, Phil. Mag. 7, 1457-1485, 1962.

Sands, M., Low Energy Mesons in the Atmosphere, Phys. Rev., 77, 180-193, 1950.

Sanlon, J. H. and S. N. Milford, Energy Spectra of Electrons from π-μ-e Decoys in Interstellar Space, Astrophys. J., 141, 718-729, 1965.

Subramanyan, A. and S. D. Verma, Intensity Distribution of High Energy Pions in the Atmosphere, Nuovo Cimento 13, 572-590, 1959.

Tulinov, V. E., A Study of Slow μ-Mesons in the Stratosphere by the Method of Delayed Coincidences, Soviet Physics, JETP, 6, 894-896, 1958.

Verma, S. D., Measurement of the Charged Splash and Reentrant Albedo of the Cosmic Radiation, (to be published, 1966).

Vogt, R. (unpublished results, 1962).

Waddington, C. J. and P. S. Freier, Electron, Hydrogen and Helium Nuclei of Cosmic Radiation, Int. Conf. on Cosmic Rays, (London), 1965.

Wolfendale, A., High Energy Muons, Proceed. Int. Conf. on Cosmic Rays. (Jaipur, India), 6, 3-21, 1963.

FIGURE CAPTIONS

Figure 1. The differential energy spectrum of primary protons at top of the atmosphere near solar minimum.

Figure 2. The multiplicity of charged π -meson production as a function of the proton kinetic energy. (The dashed lines show the uncertainty in the experimental data.)

Figure 3. Schematic diagram showing the geometry used in the calculation.

Figure 4. The production spectrum of charged π -mesons.

---Calculations of A. Subramanyan and S. D. Verma, (1959)

-.-.-. Calculations of J. Pine, et al. (1959)

__ ·· __ ·· __ ·· Calculations of Y. Tanaka (private communication 1965)

_____ Present calculations

Figure 5. The differential energy spectra of secondary electrons produced by π^+-mesons at 1 g/cm^2 atmospheric depth over Churchill, Sioux Falls, Palestine, and Hyderabad.

Figure 6. The differential energy spectra of secondary electrons produced by π^o-mesons (full curves) and by Dalitz pairs (dashed curves) at 1g/cm^2 atmospheric depth over Churchill, Sioux Falls, Palestine, and Hyderabad.

Figure 7. The differential energy spectra of all secondary electrons of different atmospheric depths over Churchill, Canada.

Figure 8. The differential energy spectra of secondary electrons at several atmospheric depths over Sioux Falls, South Dakota.

Figure 9. The differential energy spectra of secondary electrons at several atmospheric depths over Palestine, Texas.

Figure 10. The differential energy spectra of secondary electrons at several atmospheric depths over Hyderabad, India.

Figure 11. Measured electron flux from 10 to 100 MeV and from 100 to 1100 MeV vs. depth over Palestine, Texas (Sept. 1965). ____ calculated secondary electron flux; _____._____. calculated incident vertical flux (matched with experimental value 4 g/cm^2): ---- sum of the calculated secondary flux and the incident flux (re-entrant albedo).

Figure 12. Measured electron flux from 10 MeV to 100 MeV and from 100 to 1100 MeV vs. depth over Sioux Falls, South Dakota (March 1962). _____calculated secondary electron flux; ____ ____ ____ ____ calculated incident vertical flux (matched with experimental values at 3.4 g/cm^2); ---- sum of the calculated secondary flux and the incident flux (re-entrant albedo).

Figure 13. Measured electron flux between 10 MeV and 1100 MeV vs. depth over Fort Churchill, Canada (Sept. 1960). _____ calculated secondary electron flux; ____ ____ ____ ____ calculated incident vertical flux (matched with the experimental value at about 3 g/cm^2; ---- sum of the calculated secondary electron flux and the incident flux (primary).

Figure 14. Measured electron flux from 230 to 400 MeV and from 400 to 4900 MeV vs. depth over Fort Churchill (July, 1965). _____ calculated secondary electron flux; _____ _____ _____ _____ calculated incident vertical flux (matched with the experimental value at 4 ~ 5 g/cm^2): ---- sum of the calculated secondary flux and incident flux (primary).

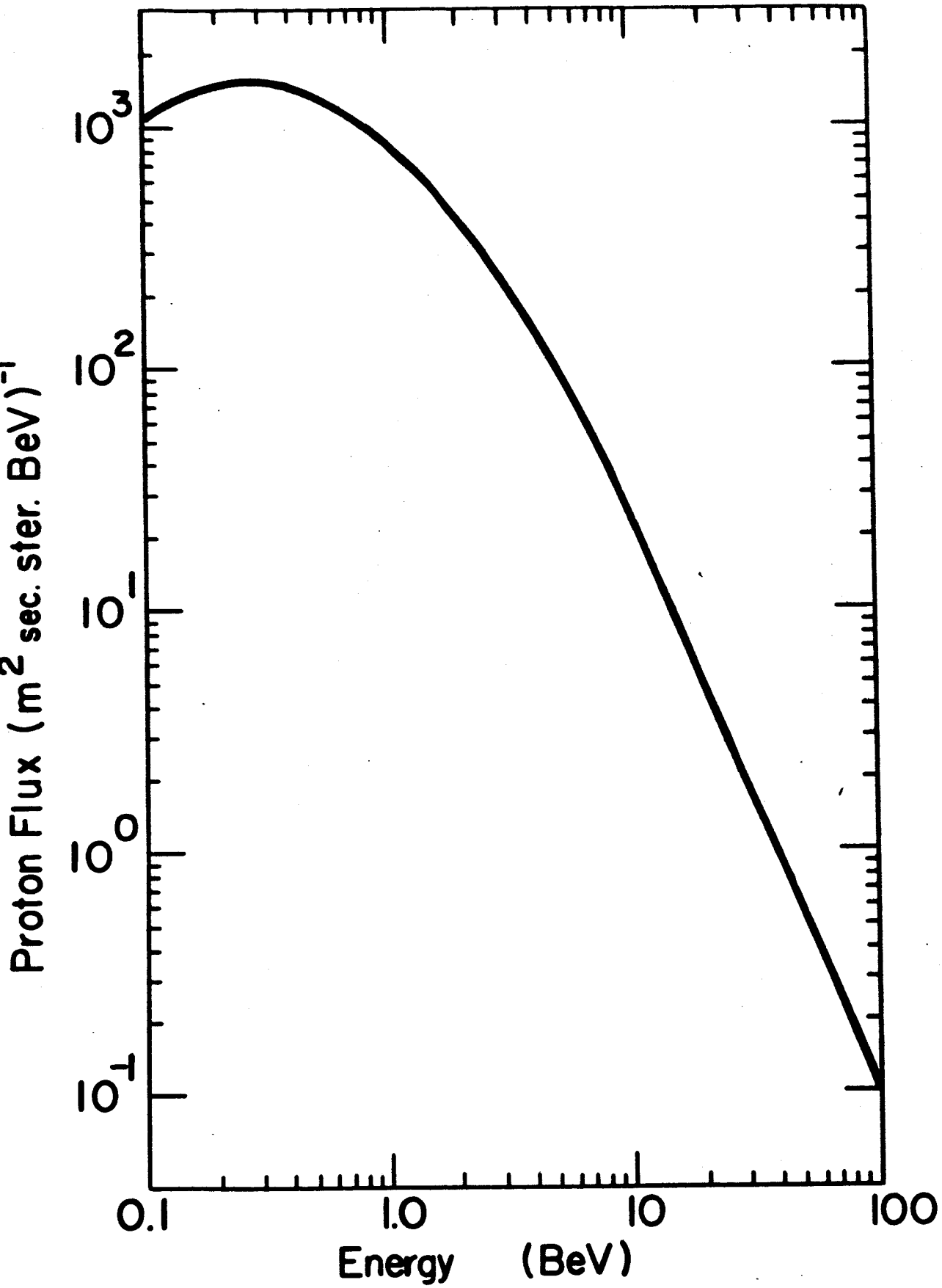
Proton Flux (m^2 sec. ster. BeV)$^{-1}$
10^3
10^2
10^1
10^0
10^{-1}
0.1
1.0
10
100
Energy (BeV)

Fig. 1

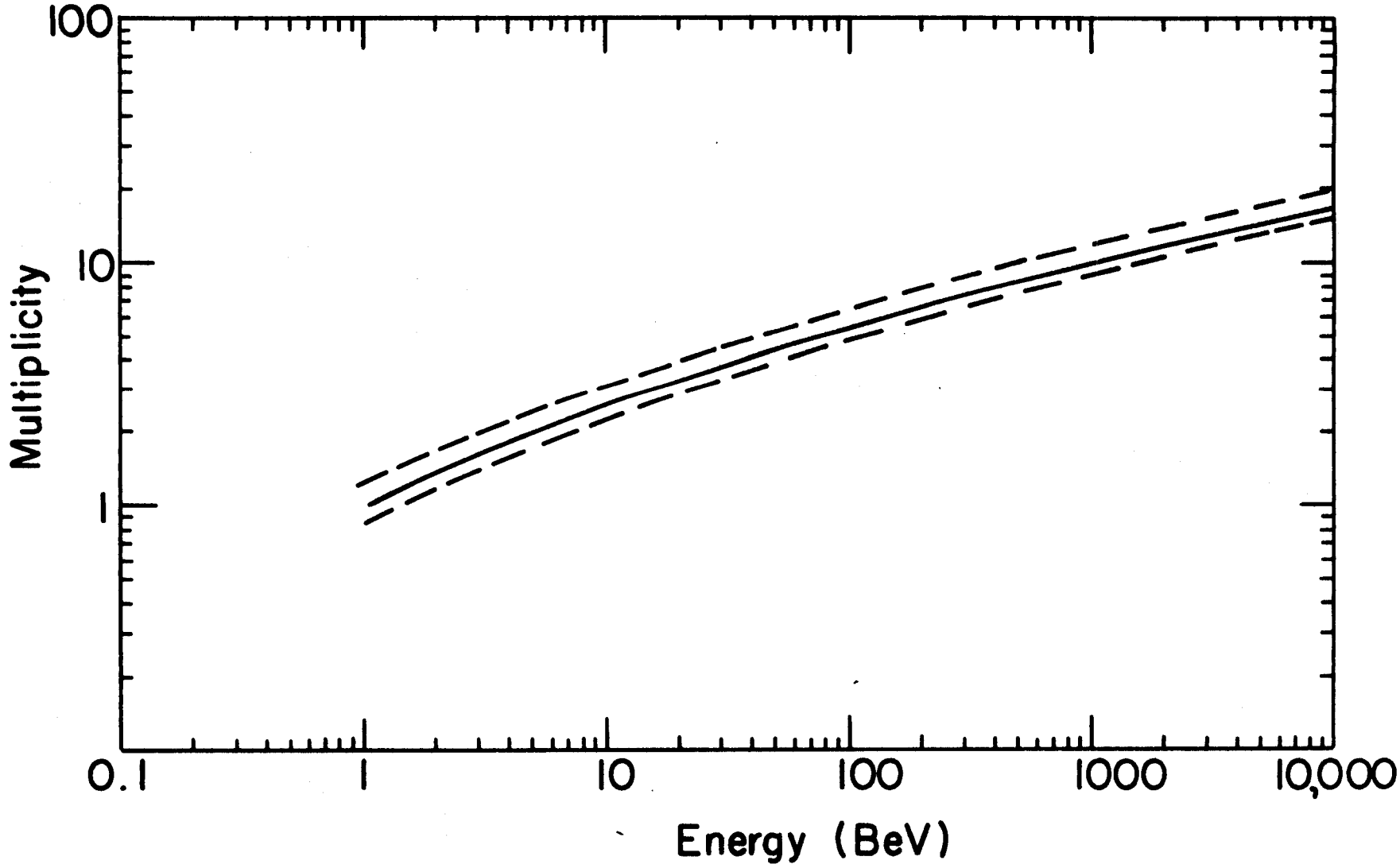

Fig. 2

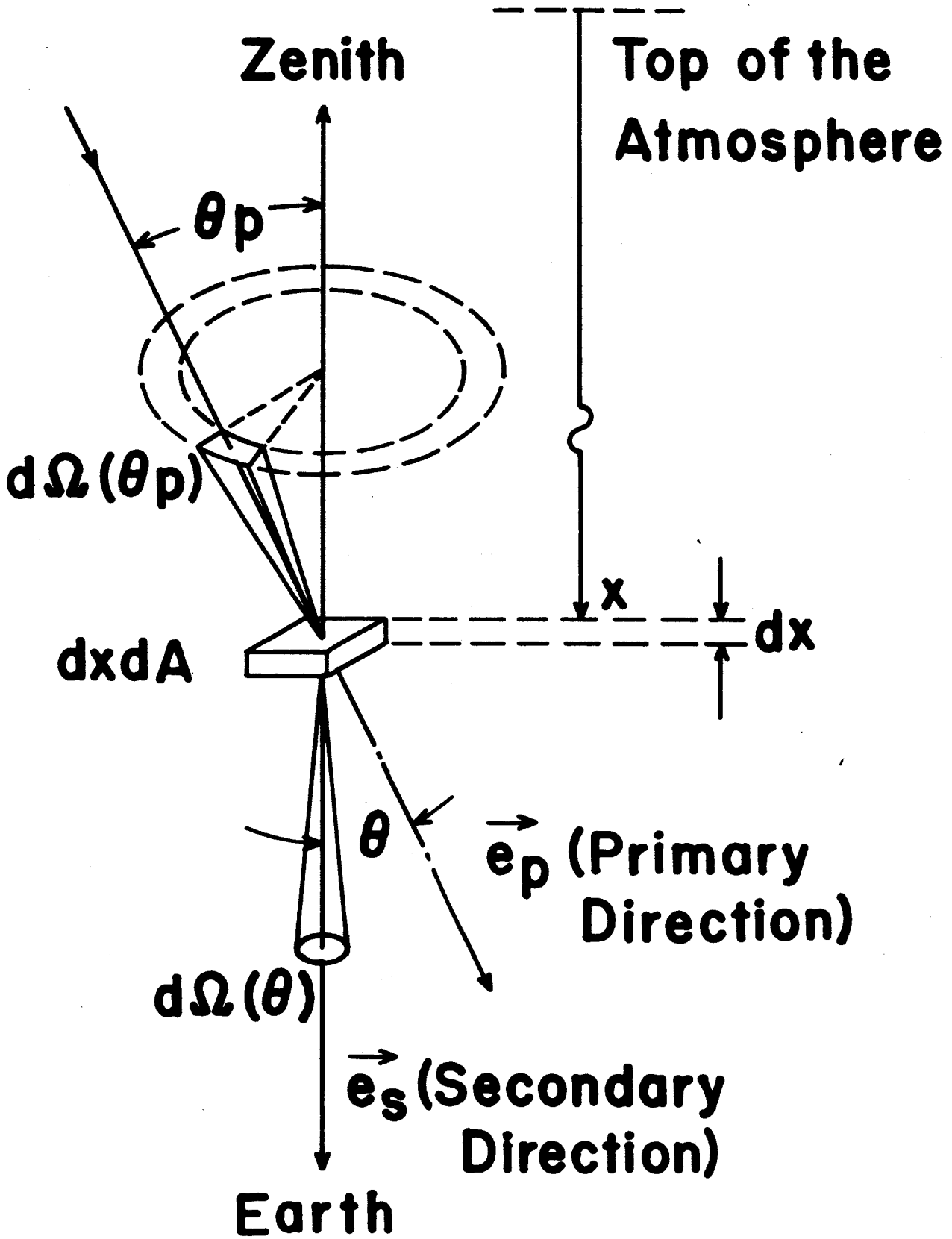
Zenith
Top of the Atmosphere
θp
dΩ(θp)
x
dx
dxdA
θ
$\vec{e}_p$ (Primary Direction)
dΩ(θ)
$\vec{e}_s$ (Secondary Direction)
Earth

Fig. 3

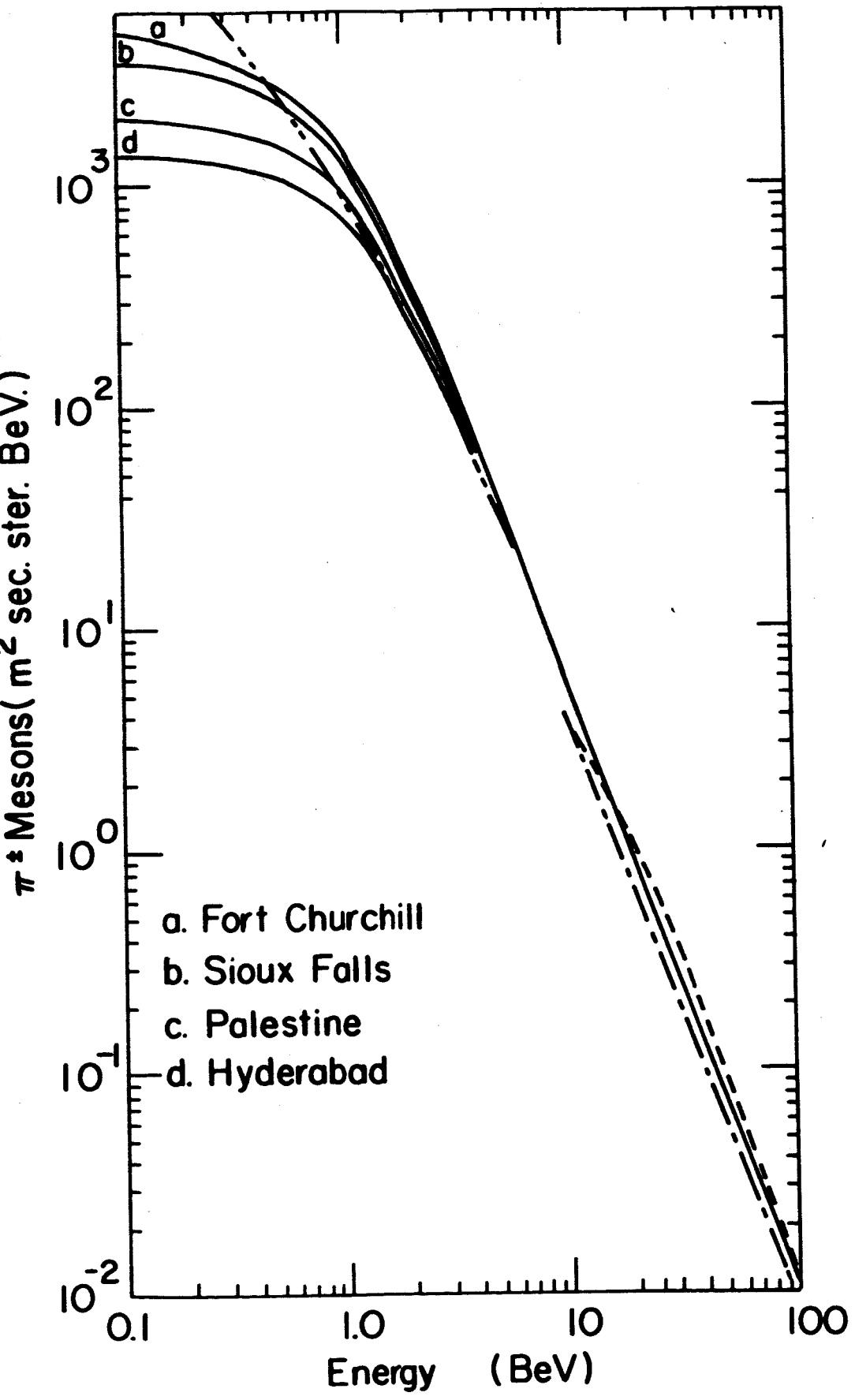
a
b
c
d
10^3
10^2
10^1
10^0
10^{-1}
10^{-2}
$\pi^{\pm}$ Mesons(m^2 sec. ster. BeV.)$^{-1}$
a. Fort Churchill
b. Sioux Falls
c. Palestine
d. Hyderabad
0.1
1.0
10
100
Energy (BeV)

Fig. 4

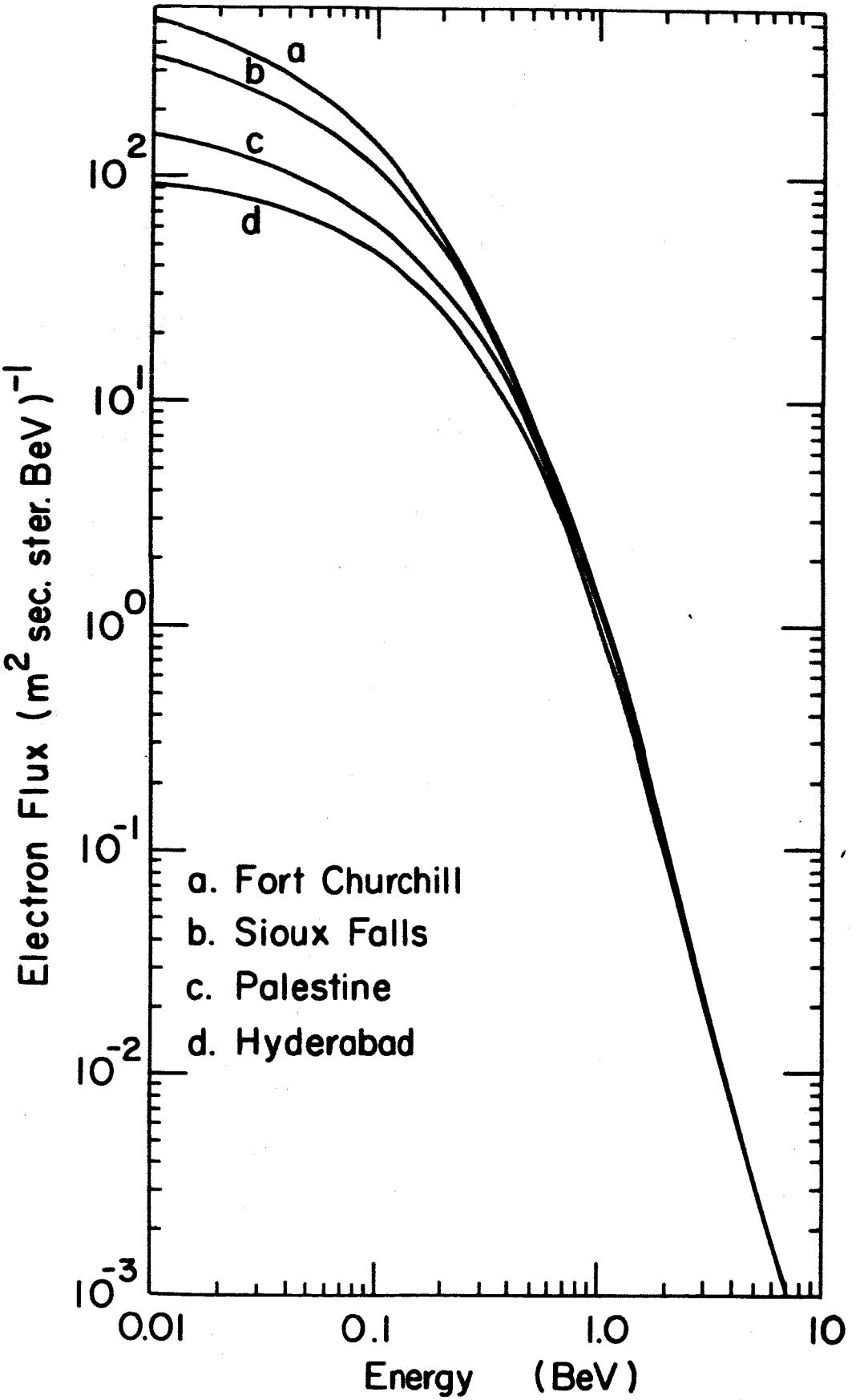
a
b
c
d
10^2
10^1
10^0
10^{-1}
10^{-2}
10^{-3}
Electron Flux (m^2 sec. ster. BeV)$^{-1}$
a. Fort Churchill
b. Sioux Falls
c. Palestine
d. Hyderabad
0.01
0.1
1.0
10
Energy (BeV)

Fig. 5

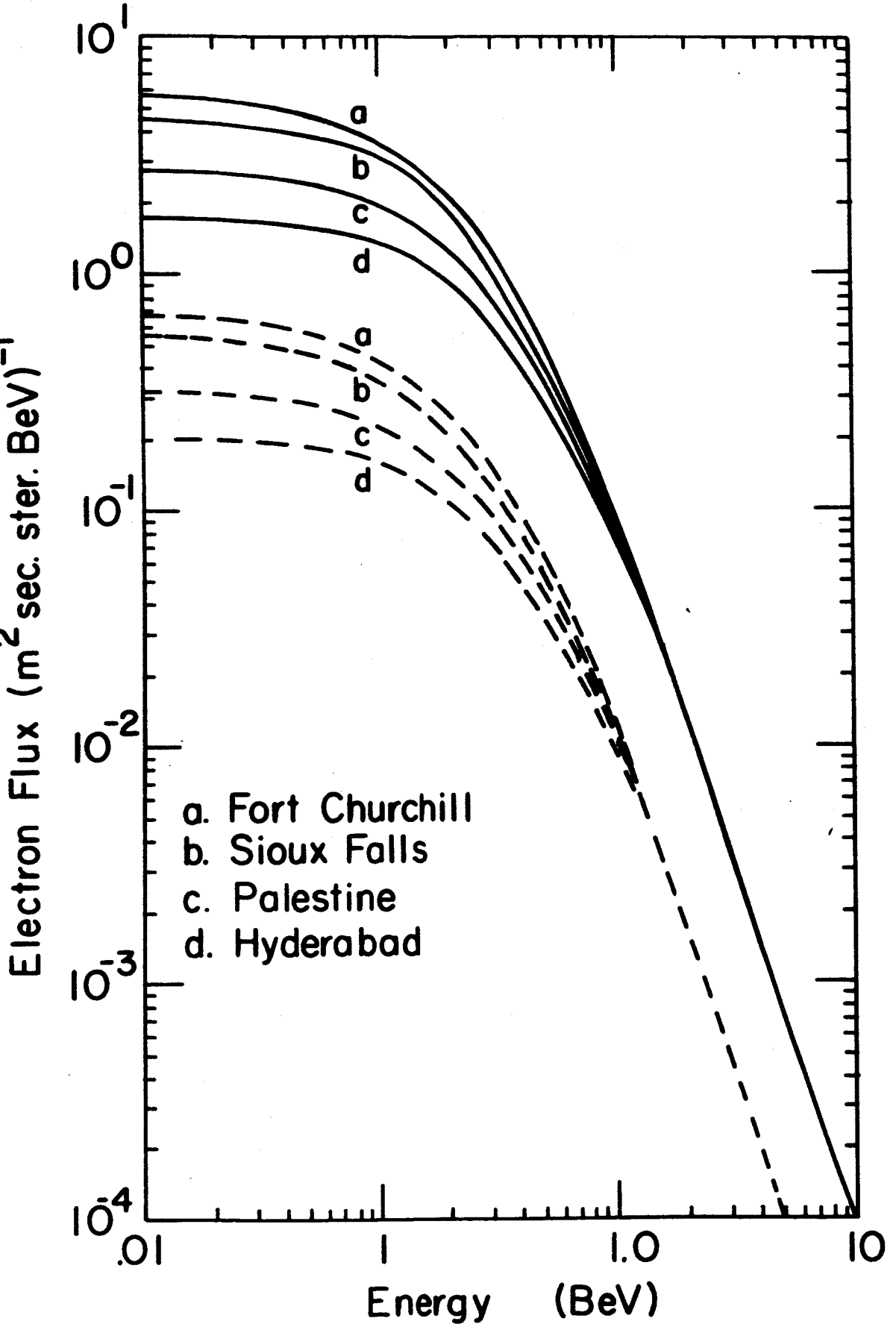
Electron Flux (m^2 sec. ster. BeV)$^{-1}$
10^1
10^0
10^{-1}
10^{-2}
10^{-3}
10^{-4}
a
b
c
d
a
b
c
d
a. Fort Churchill
b. Sioux Falls
c. Palestine
d. Hyderabad
.01
1
1.0
10
Energy (BeV)

Fig. 6

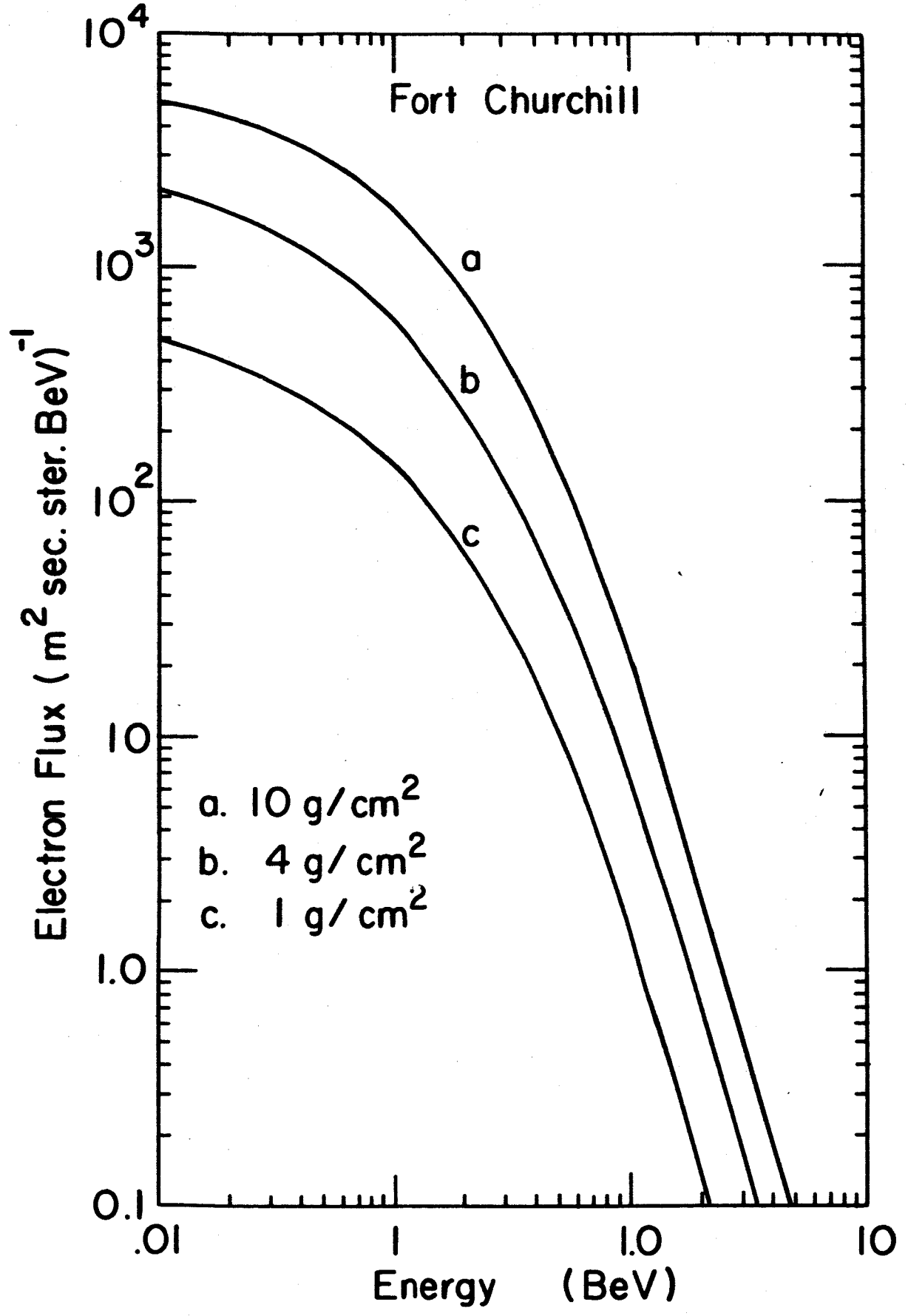
Fort Churchill
Electron Flux (m^2 sec. ster. BeV)$^{-1}$
10^4
10^3
10^2
10
1.0
0.1
a
b
c
a. 10 g/cm^2
b. 4 g/cm^2
c. 1 g/cm^2
.01
1
1.0
10
Energy (BeV)

Fig. 7

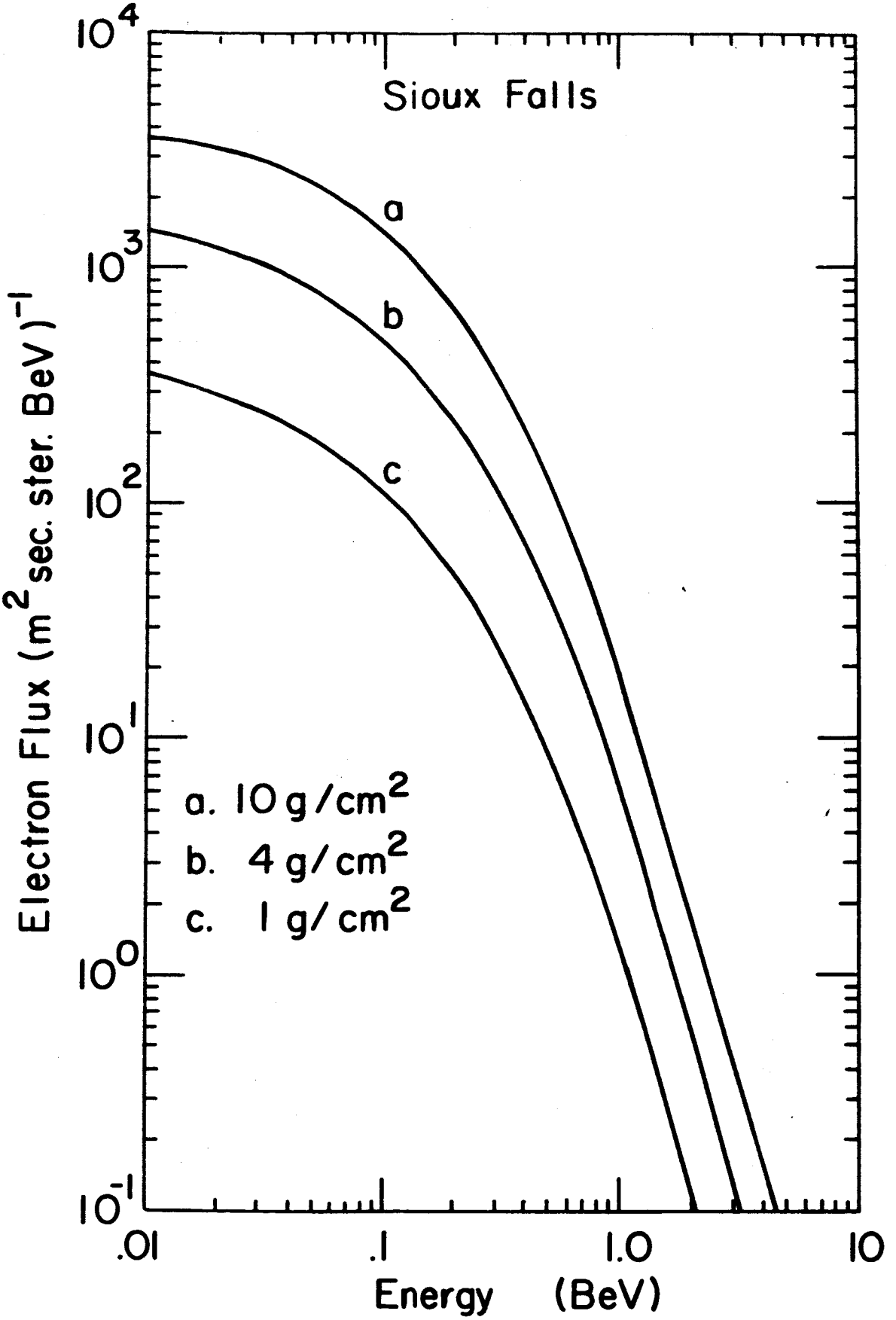
Sioux Falls
Electron Flux (m^2 sec. ster. BeV)$^{-1}$
10^4
10^3
10^2
10^1
10^0
10^{-1}
a
b
c
a. 10 g/cm^2
b. 4 g/cm^2
c. 1 g/cm^2
.01
.1
1.0
10
Energy (BeV)

Fig. 8

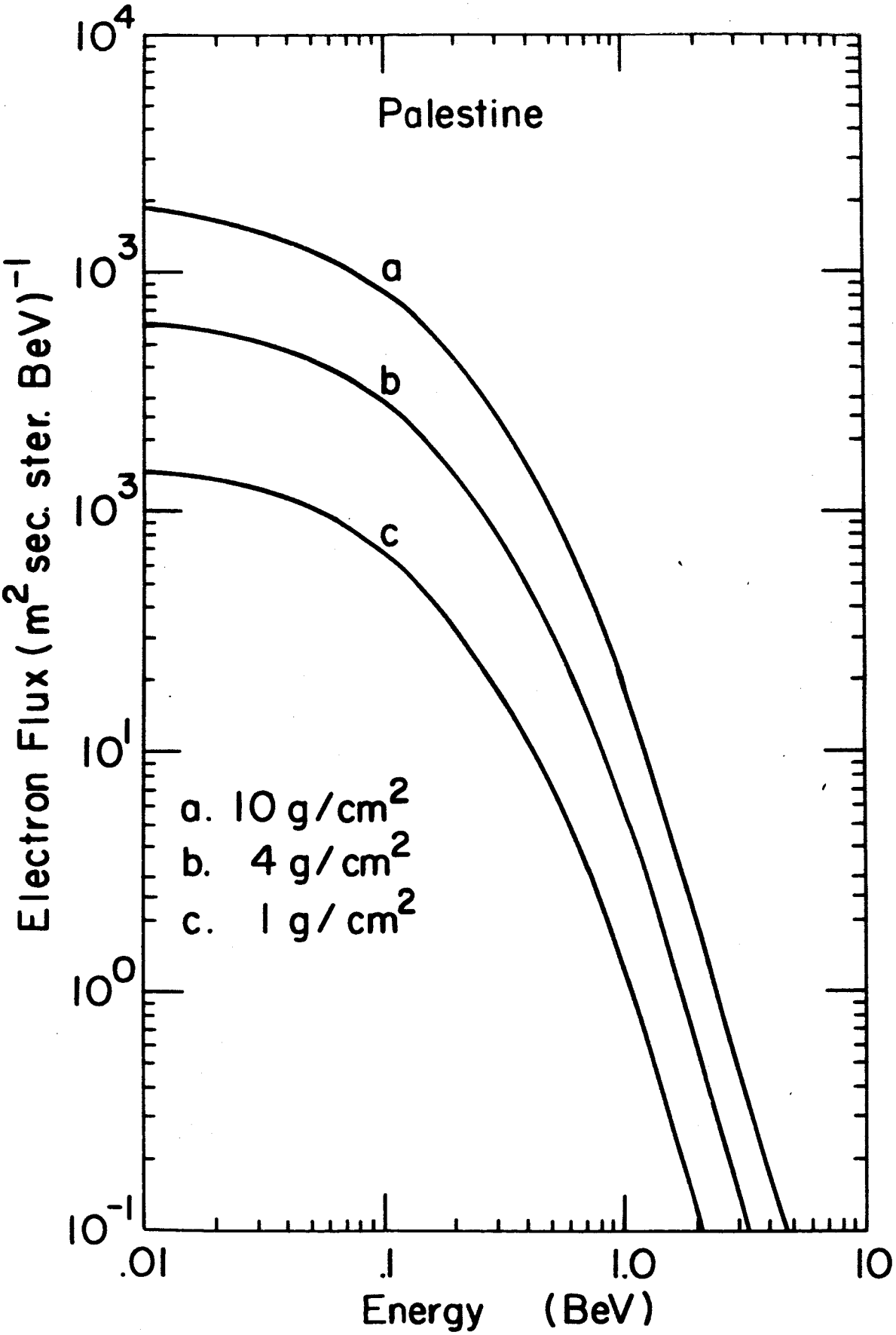
Palestine
Electron Flux (m^2 sec. ster. BeV)$^{-1}$
10^4
10^3
10^3
10^1
10^0
10^{-1}
a
b
c
a. 10 g/cm^2
b. 4 g/cm^2
c. 1 g/cm^2
.01
.1
1.0
10
Energy (BeV)

Fig. 9

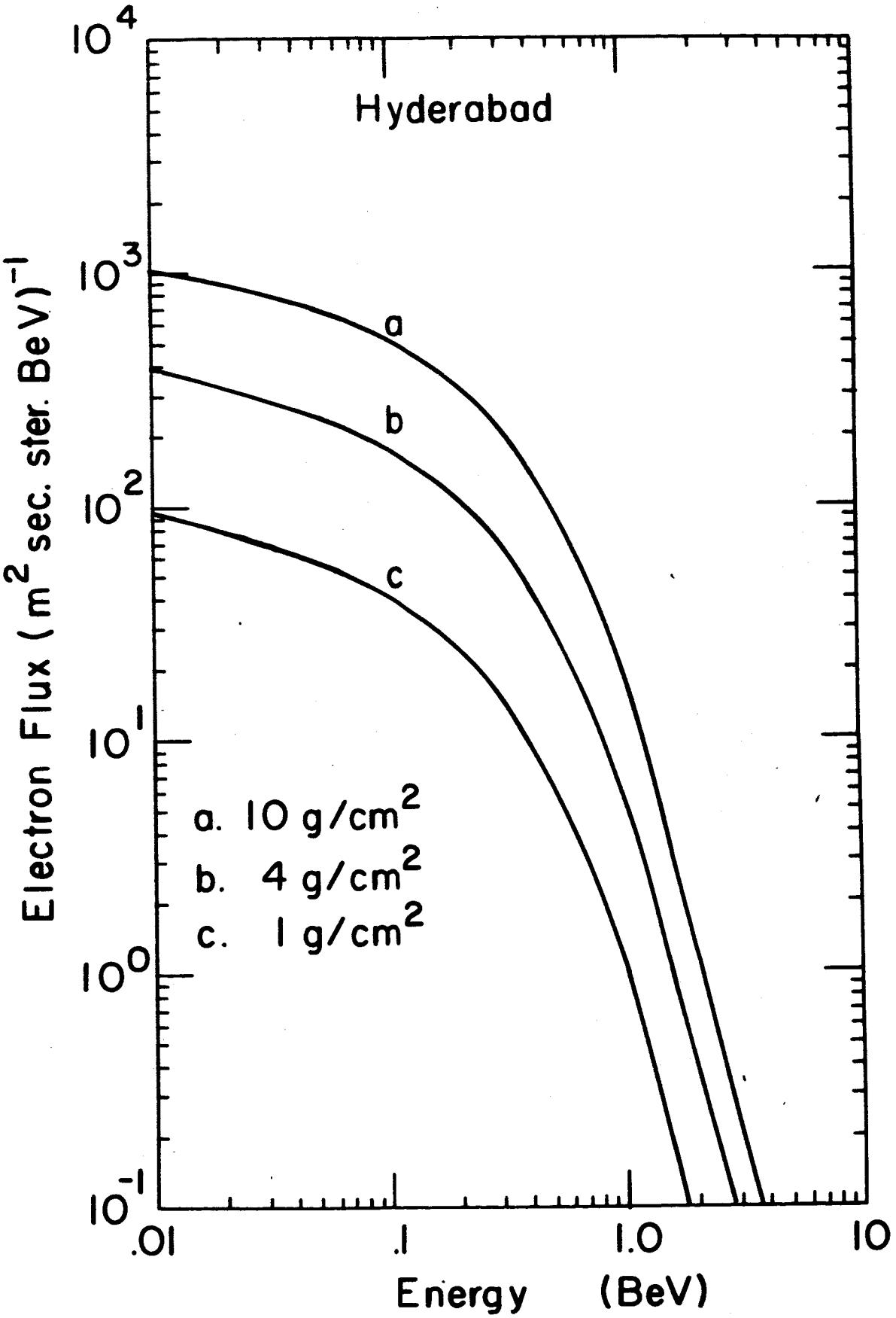
Hyderabad
Electron Flux (m^2 sec. ster. BeV)$^{-1}$
10^4
10^3
10^2
10^1
10^0
10^{-1}
a
b
c
a. 10 g/cm^2
b. 4 g/cm^2
c. 1 g/cm^2
.01
.1
1.0
10
Energy (BeV)

Fig.10

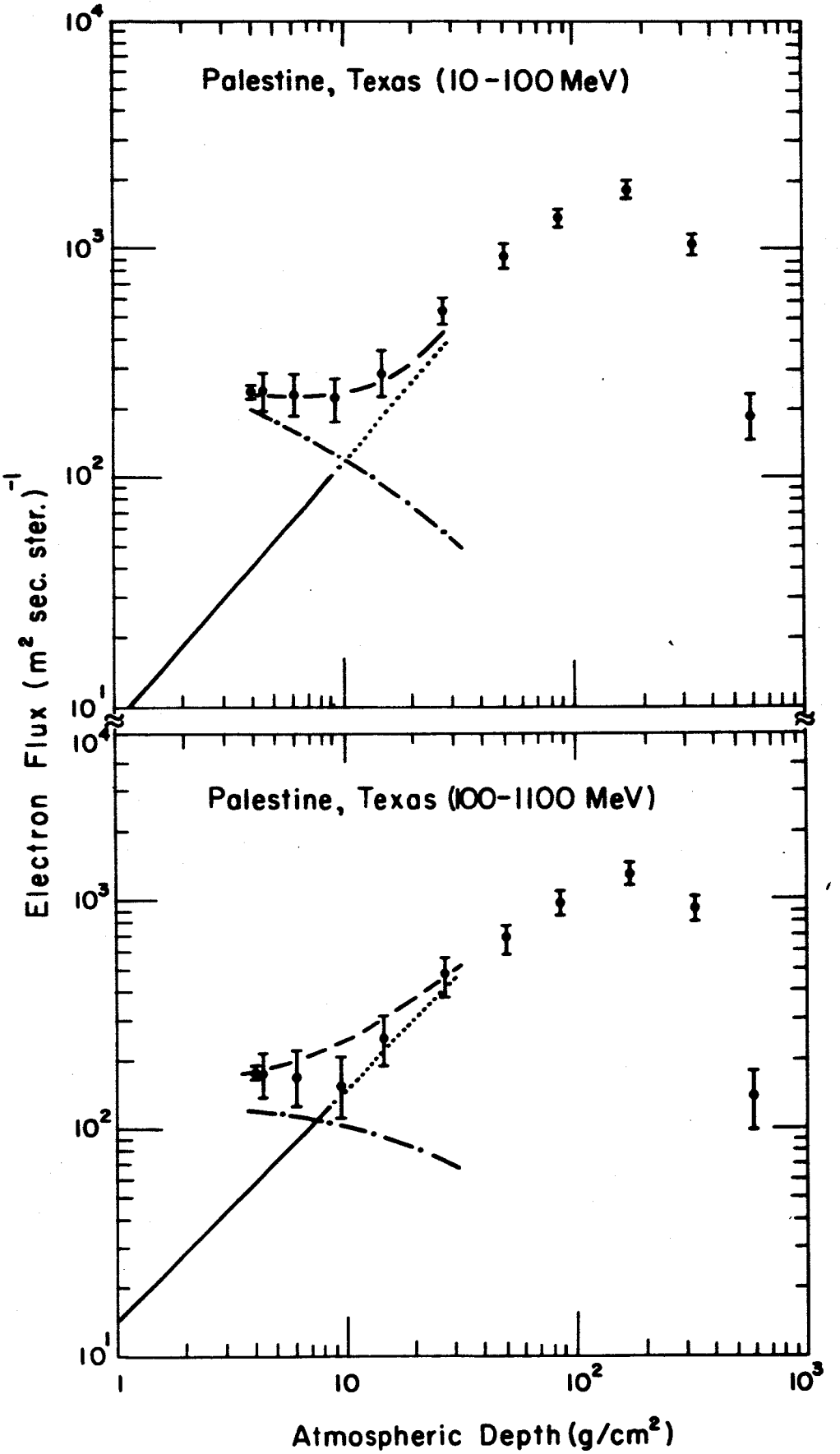
Palestine, Texas (10-100 MeV)
Palestine, Texas (100-1100 MeV)
Electron Flux (m² sec. ster.)⁻¹
Atmospheric Depth (g/cm²)
10⁴
10³
10²
10¹
1
10
10²
10³

Fig.11

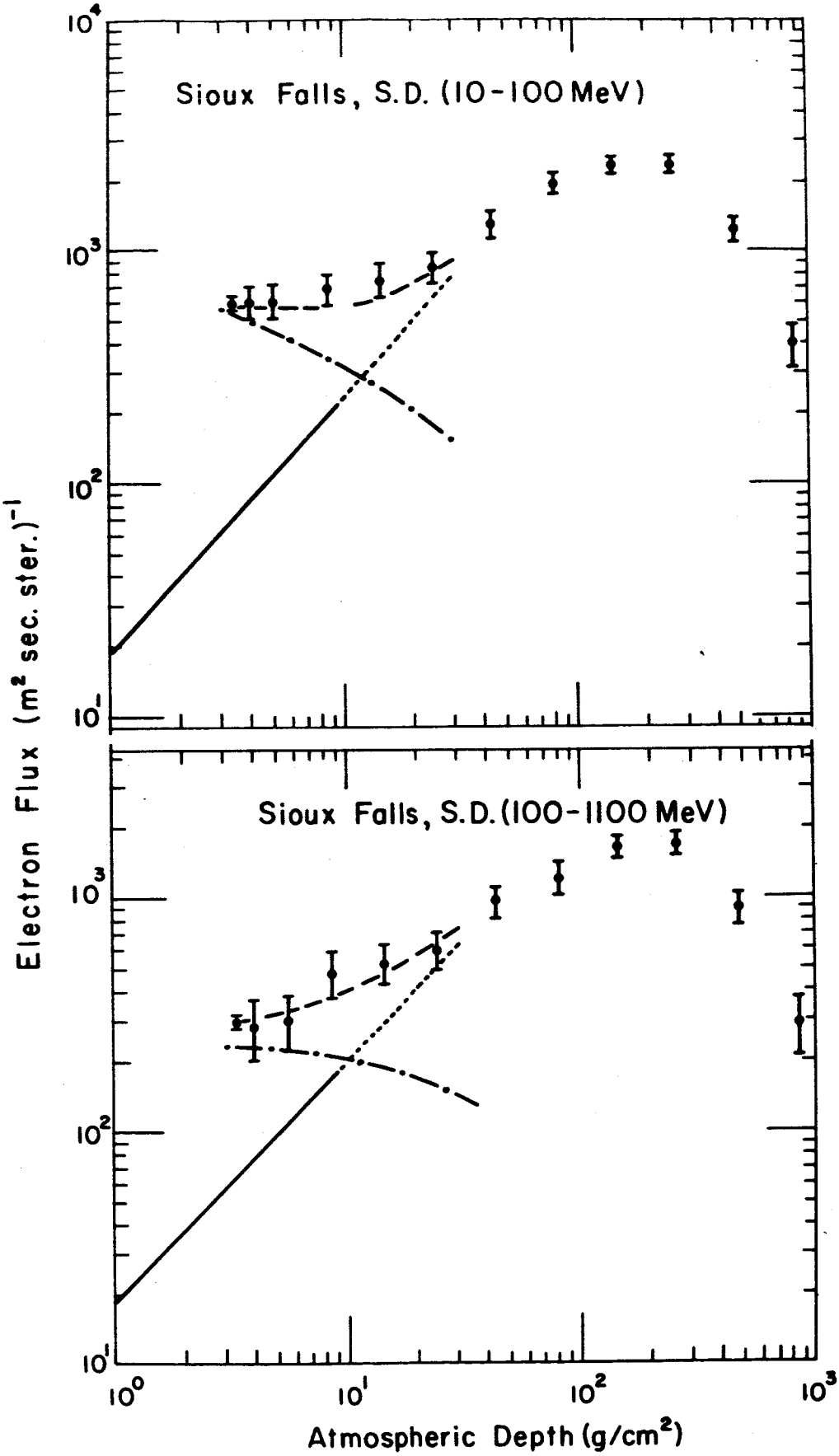
Sioux Falls, S.D. (10-100 MeV)
Sioux Falls, S.D. (100-1100 MeV)
Electron Flux (m² sec. ster.)⁻¹
Atmospheric Depth (g/cm²)
10⁴
10³
10²
10¹
10⁰
10¹
10²
10³

Fig. 12

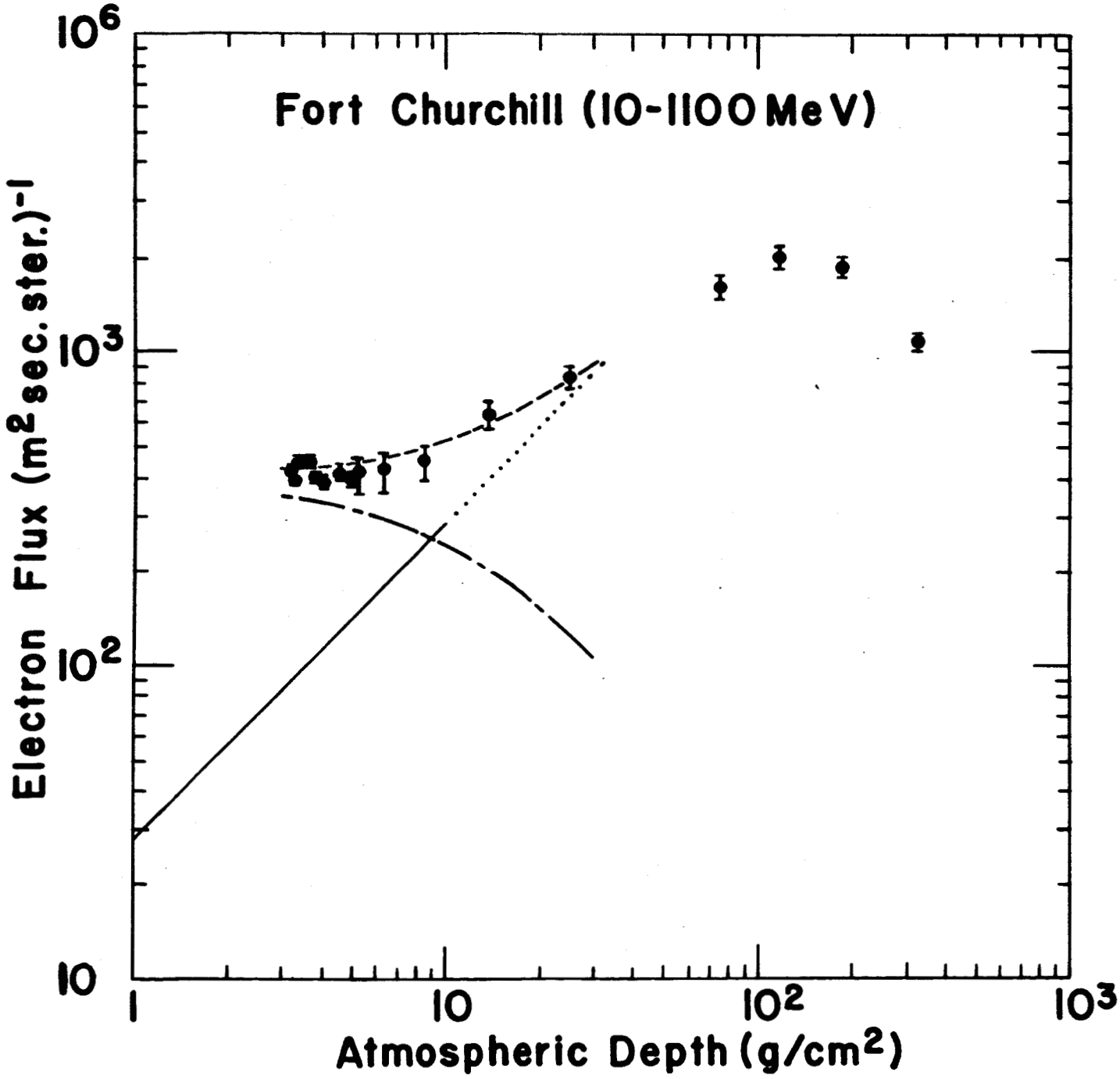
Fort Churchill (10-1100 MeV)
Electron Flux (m² sec. ster.)⁻¹
Atmospheric Depth (g/cm²)
10⁶
10³
10²
10
1
10
10²
10³

Fig.13

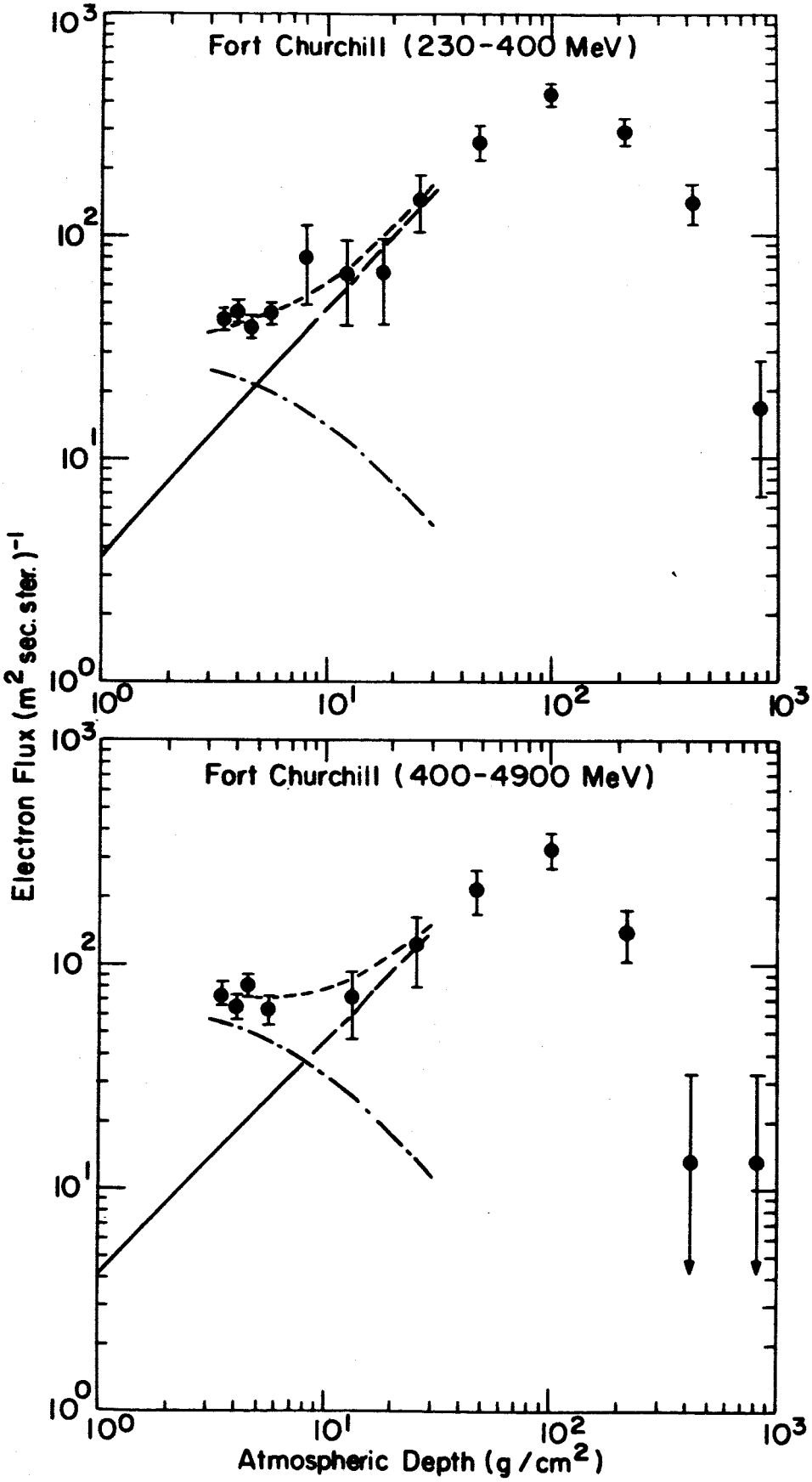
Fort Churchill (230-400 MeV)
Fort Churchill (400-4900 MeV)
Electron Flux (m² sec. ster.)⁻¹
Atmospheric Depth (g/cm²)
10⁰
10¹
10²
10³

Fig. 14